POSTER REFERENCE: ICF10033PR

EXPERIMENTAL-NUMERICAL ANALYSIS OF MECHANISMS OF DAMAGE INITIATION IN TOOL STEELS

L. Mishnaevsky Jr [1], N. Lippmann [2] and S. Schmauder [1]

[1] Staatliche Materialprüfungsanstalt (MPA), University of Stuttgart
Pfaffenwaldring 32, 70569 Stuttgart, Germany
Email: Leon.Mishnaevsky@mpa.uni-stuttgart.de

[2] Robert Bosch GmbH, FV/PLM, D-70442 Stuttgart, Germany

ABSTRACT

SEM in-situ investigations of the micromechanisms of damage initiation and fracture in tool steels are described. The critical state of the material and the damage growth were observed in the tests. It was shown that the initial microcracks in the steels are formed in primary carbides and then join together. A hierarchical finite element model of damage initiation, which included a macroscopic model of the deformation of the specimen under real experimental conditions and a mesomechanical model of damage in real microstructures of steels was developed. Using the hierarchical model, the conditions of local failure in the steels have been obtained.

KEYWORDS

High speed steels, damage, fracture, micromechanics, microstructure, finite elements, in-situ experiments

INTRODUCTION

The improvement of service properties of tool steels presents an important source of increasing the efficiency of metalworking industry. In order to develop a numerical model of damage or fracture in the steel, which should serve to predict the lifetime of the steel tool, or to improve the steel properties, one needs to know the mechanisms of damage and fracture in the steels [1-3]. The direct in-situ observation of the fracture mechanisms of the steels under microscope is quite difficult as compared with the case of more ductile materials, since the material fails very quickly. Then, not only qualitative parameters of fracture (like its mechanisms) but also quantitative ones (like critical damage parameters) are of interest. The purpose of this work was to study the mechanisms and conditions of damage initiation and growth in the tool steels both qualitatively and quantitatively. The work includes the following steps:

- SEM-in situ experiments on 3-point bending of specimens with inclined notches,
- FE-Simulation of the deformation of the specimens on macro- and mesolevel, taking into account the real microstructure of the steels observed in the SEM-experiments.

The SEM in-situ observation of the damage initiation allowed to clarify the micromechanisms of damage initiation, whereas the developed hierarchical finite element model (macro- and mesomodel) made it possible to determine the failure conditions for steels constitutents using the real loading conditions and real microstructure of the steel.

SEM IN-SITU INVESTIGATIONS OF MICROMECHANISMS OF DAMAGE INITIATION

Conditions of Experiments

In order to clarify the mechanisms of damage initiation and growth in the steels, a series of SEM-in-situ-experiments was carried out. 3-point bending specimens with an inclined notch, as described in [4], were used in these tests. These specimens allow to observe the micro- and mesoprocesses of local deformation and failure of carbides and the matrix of steels during loading of macroscopic specimens in the SEM. The shape and sizes of the specimens are shown schematically in Figure 1. The advantage of the specimen with the inclined notch is that the most probable location of first microcrack initiation in the specimen notch can be simply predicted (which is not the case for the usual 3-point bending specimens). Therefore, one can observe this place with high magnification during loading and identify the load and the point in time at which the first microcracks form very exactly. Specimens made from the cold work steel X155CrVMo12-1 (in further text denoted as KA) and high speed steel HS6-5-2 (denoted as HS) have been used. In the experiments, the specimens with different orientations of primary carbide layers were studied. Since the tool steels are produced in the form of round samples and was subject to hot reduction after austenitization and quenching, they are anisotropic: the carbide layers are oriented typically along the axis of the cylinder (this is the direction of hot reduction). Therefore, the following designation of the specimen orientation was used: L – the direction along the carbide layers, R – radial direction in the workpiece, C – the direction along the workpiece axis. In the experiments, specimens with orientations CL, LC and CR have been used. The CR and CL specimens are shown in Figure 2. The specimens have been subjected to the heat treatment (hardening at 1070^{o}C in vacuum and tempering 2 times at 510^{o}C), and then polished with the use of the diamond pastes of different sizes till the roughness R_z of the surface of the specimens does not exceed 3 μm. The notch region of the specimens was etched with 3 % and 10 % HNO_3 until the carbides were seen on the surface.

Then, the specimens have been subjected to loading with simultaneous observation of the notch region in SEM. The scheme of loading is given in Figure 1 as well. Each loading test was repeated 3 times for each type of steel and specimen orientation.

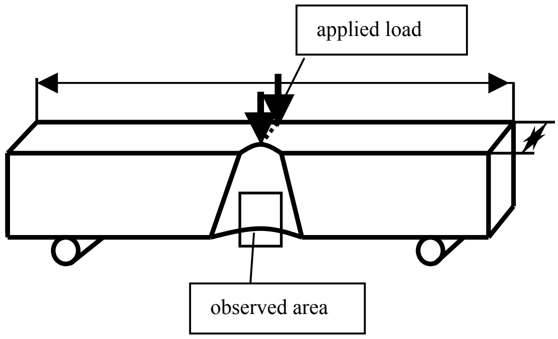

Figure 1. 3-point bending specimens

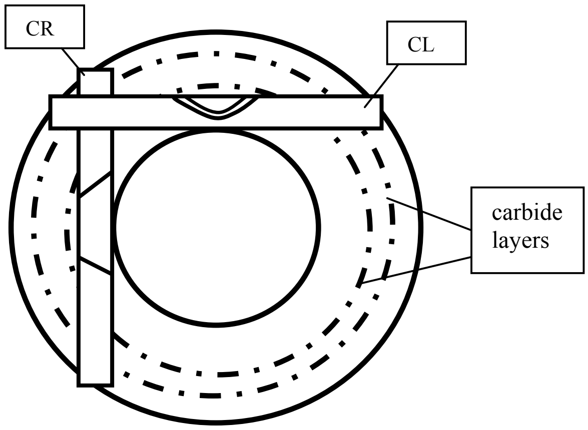

Figure 2. Orientation of CR and CL specimens as related to the carbide layers

Results of the Experiments

The force-displacement curves were recorded during the tests. The loading was carried out in small steps, with the rate of loading about 1 mm/s. The places in the specimen notch where the microcrack initiation was expected have been observed through scanning electron microscopy (SEM) during the tests. It was observed that the first microcracks formed only in the primary carbides, and not in the "matrix" of the steel. Also, no microcrack along the carbide/matrix interface was observed in the tests. The forces at which the failure of primary carbides was observed in each specimen are given in the Table 1.

TABLE 1. CRITICAL FORCES IN THE EXPERIMENTS .

Numbers of specimens	Type of the specimen	Force at which first microcrack was observed in the specimen, N	Force at which the specimen failed, N
1-3	KALC	95, 52, 37.5	155, 85,160
4-6	KACR	50, 55, 37.5	95, 95, 70
7-9	HSCR	45, 50 (several microcracks in both large and small carbides), 50	95, 80, 95
11-12	HSLC	50 (one microcrack), 72.5 (another microcrack), 127	200, 190, 195

Generally, the course of failure of the specimens was as follows: (1) formation of a microcrack at some carbide, (2) formation of several microcracks at many carbides in different places of observed area (in so doing, the microcracks are formed rather at larger carbides at some distance from the boundary of the specimen, than in more strained macroscopically areas in the vicinity of the lower boundary of the specimen; the local fluctuations of stresses caused by the carbides have evidently much more influence on the microcracking than the macroscopic stress field), and (3) after the failure of many carbides, the microcracks (or plastic zones in front of the microcracks) begin to grow into the matrix; just after this occurs, the specimens fail. The failure of many carbides was observed just before the specimens failed. The differences between the loads at which the microcracks are formed, and that at which the specimen failed was in most cases very small. Figure 3 shows the SEM micrographs of a typical primary carbide in the notch region of steels before and after its failure. Comparing the values of critical forces from Table 1, one may conclude that the failing force for the specimens with orientation LC is much higher than with the orientation CR (more than twice). Then, the force at which first microcracks form and first carbides fail depends on the orientation of specimens much more for high speed steels than for the cold work steels.

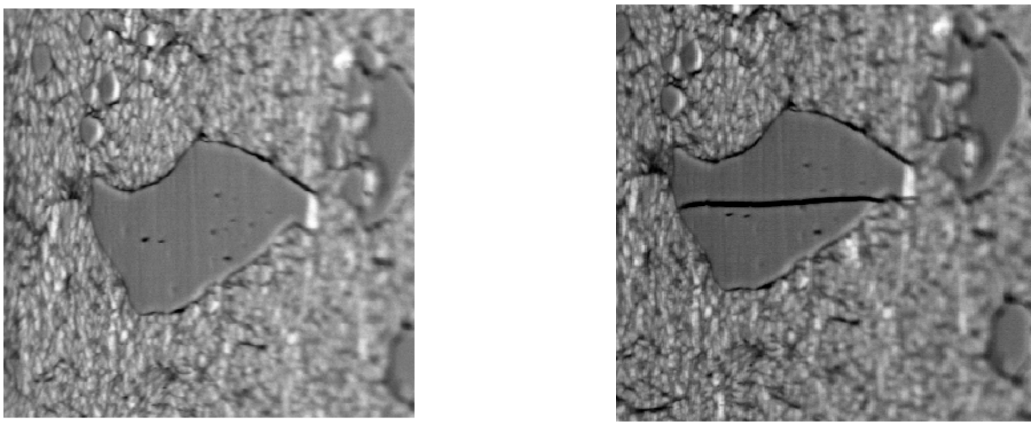

a) b)

Figure 3. A carbide grain before (a) and after failure (b). (Area size 40x100 μm).

MESOMECHANICAL SIMULATION OF DEFORMATION IN STEELS

To simulate the deformation of 3-point bending specimens with inclined notch, a three-dimensional FE model of the specimen was developed. Due to the symmetry of the specimen, only one half of the specimen was taken. The material was assumed to be homogeneous. The forces measured in the tests described above were applied in the simulations. The displacements from the boundary nodes of elements which are located in the vicinity of the symmetry plane and at the lower notch boundary are used as boundary conditions in the mesomechanical simulation of carbide failure. Then, the 2D mesomechanical simulations of carbide failure have been carried out for each microstructure and each load, measured in the experiments. The 2D-model was created, which represents the cluster of finite elements in the notch region of the specimen. The real structure region with 5000 elements of the plane strain type TRIP 6 and size 100 μm x 100 μm was located in the lower left corner of the model. As boundary conditions the displacements from the model of deformation of 3-point bending specimen were taken. Since the mesh density in the 2D case is higher, the calculated displacements have been linearly interpolated between the points which were available in the 3D simulation.

The mesomechanical simulation was performed with the use of the multiphase element method [5]. The micrograph of the carbide, obtained in SEM-in-situ experiments was digitized, and then automatically imposed on the region of the real structure. The micrographs to be digitized were chosen in such a way that they were representative enough for the given materials. Due to the inclined notch surface, the micrographs in Figure 3 have different scales in X- and Y-directions. To take that into account, the micrographs were scaled with the use of the image analysis software XView accordingly to their scales in both directions. The properties of carbide and matrix are as follows [3, 4, 6, 7]: (cold work steel) E_C=276 GPa, E_M=232 GPa, constitutive law of the matrix: $\sigma_y = 1195 + 1390\ [1-\exp(-\epsilon_{pl}/0.0099)]$; (high speed steels) E_C=286 GPa, E_M=231 GPa, constitutive law of the matrix: $\sigma_y = 1500 + 471\ [1-\exp(-\epsilon_{pl}/0.0073)]$, Poisson's ratio - 0.19 (carbides) and 0.3 (matrix).

FAILURE STRESS OF PRIMARY CARBIDES

Figure 4 gives the distribution of von Mises stress in the real microstructure of the cold work steel at the loads at which the carbide failed. Supposing that failure of the carbides is determined by the action of maximal normal stresses, one obtains the failure stresses of carbides for different steels and orientations (see Table 2).

TABLE 2. FAILURE STRESS OF CARBIDES

Type of the steel	KALC	KACR	HSCR	HSLC
Failure stress of carbides, MPa	1826	1840	1604	2520

It is of interest to compare the above results with some literature data. Lippmann et al. [8] and Lippmann [4] obtained the values 1863...1987 and 1200...2100 MPa, respectively, for the failure stress of carbides in cold work and high speed steels. One can see that our values for cold work steels are very close to those given in [4]; the values for high speed steels are about the higher boundary of the variation range.

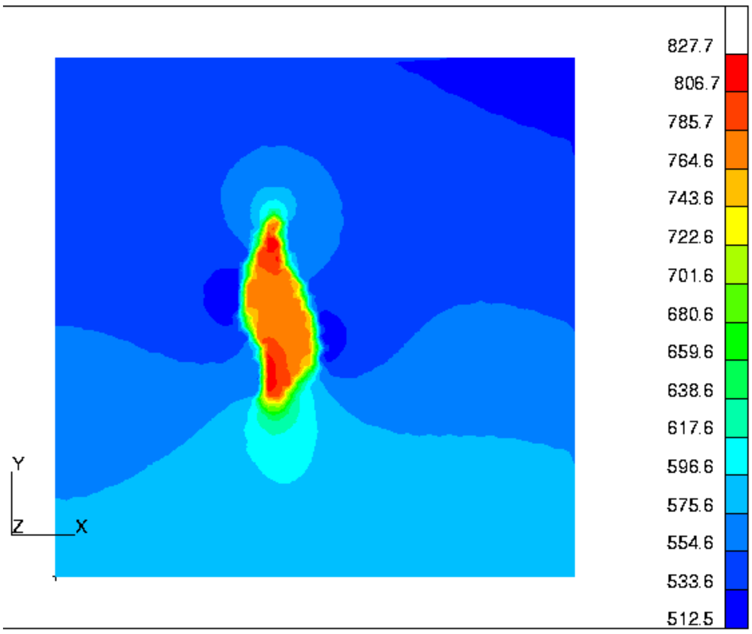

Figure 4. Von Mises stress distribution in the real microstructure of the steel in the notch of the specimen.

CONCLUSIONS

On the basis of the above analysis, one can draw the following conclusions:

1) The course of failure of the specimens was as follows: formation of one microcrack at some carbide, then formation of several microcracks at many carbides in different places of the observed area (in so doing, the microcracks are formed rather at larger carbides at some distance from the boundary of the specimen, than in more strained macroscopically

areas in the vicinity of the lower boundary of the specimen; the local fluctuations of stresses caused by the carbides have evidently much more influence on the microcracking than the macroscopic stress field), and, finally, after the failure of many carbides, the microcracks (or plastic zones in front of the microcracks) begin to grow into the matrix; just after this occurs, the specimens fail.

2) The initial microcracks in the steels are formed in primary carbides (i.e. not along the carbide/matrix interface and not in the matrix).
3) The failing force for the specimens with orientation LC is much higher than with the orientation CR (more than twice). The force at which first microcracks form and first carbides fail depends on the orientation of specimens much more for high speed steels than for the cold work steels.
4) The failure stresses of carbides (of approximately average sizes for given steels) determined from the SEM in-situ experiments and the FEM simulations are 1826 MPa (the specimen KALC), 1840 MPa (KACR), 1604 MPa (HSCR) and 2520 MPa (HSLC). The failing stress of carbides depends of the orientation of carbide layers in high speed steels much more than in cold work steels.

Acknowledgement: The authors gratefully acknowledge the financial support by the European Commission via the ECSC-Project 8834 "Influence of micromechanical mechanisms on strength and damage of tool steels under static and cyclic loading". The authors are grateful to the administration and specialists from the Technical University - Mining Academy Freiberg (TU BAF), who made it possible to carry out the SEM-in-situ experiments on their equipment and supported us during the experiments.

References

1. L. Mishnaevsky Jr and S. Schmauder (2001), *Appl. Mech. Rev*, 54, 1
2. L. Mishnaevsky Jr, N. Lippmann and S. Schmauder (2000), *In: Proc. 13th European Conference on Fracture "Fracture Mechanics : Applications and Challenges*", CD-ROM
3. L. Mishnaevsky Jr, N. Lippmann and S. Schmauder, Computational Optimization of Materials by Varying the Microstructures: Some Recent Developments as Applied to the Improvement of Fracture Resistance of Tool Steels (submitted)
4. N. Lippmann (1995), Dissertation, Freiberg, Germany
5. L. Mishnaevsky Jr, M. Dong, S. Hoenle and S. Schmauder (1999), *Comp. Mater. Sci.,* 16, 1-4, 133-143
6. L. Mishnaevsky Jr and S. Schmauder, (2000), *Influence of Micromechanical Mechanisms of Strength and Deformation of Tool Steels under Static and Cyclic Load*, ECSC RTD Project Final Report, 2000, Creusot Loire, Frankreich
7. L. Mishnaevsky Jr and S. Schmauder (1999), *Pursuance and Analysis of SEM-in-situ-Experiments on the Deformation and Fracture of Cold Work and High Speed Steels,* MPA Report, 35 pp.
8. N. Lippmann, A. Lehmann, Th. Steinkopff and H.-J. Spies (1996), *Comp. Mat. Sci*., 7, 123-130